ORNL-3067
UC-4 - Chemistry

SUPERPOSITION OF FORCED AND DIFFUSIVE FLOW IN A LARGE-PORE GRAPHITE

R. B. Evans III
J. Truitt
G. M. Watson

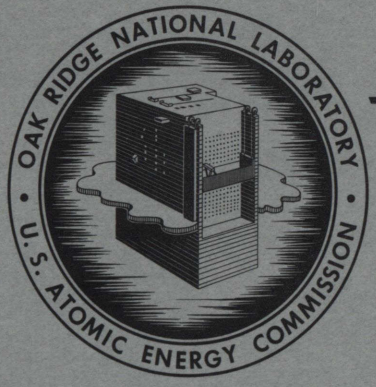

OAK RIDGE NATIONAL LABORATORY
operated by
UNION CARBIDE CORPORATION
for the
U.S. ATOMIC ENERGY COMMISSION

Printed in USA. Price $1.75. Available from the

Office of Technical Services
Department of Commerce
Washington 25, D.C.

ORNL-3067
UC-4 - Chemistry
TID-4500 (16th ed.)

Contract No. W-7405-eng-26

REACTOR CHEMISTRY DIVISION

SUPERPOSITION OF FORCED AND DIFFUSIVE FLOW IN A LARGE-PORE GRAPHITE

R. B. Evans, III, J. Truitt
and G. M. Watson

DATE ISSUED

MAR 10 1961

OAK RIDGE NATIONAL LABORATORY
Oak Ridge, Tennessee
operated by
UNION CARBIDE CORPORATION
for the
U.S. ATOMIC ENERGY COMMISSION

CONTENTS

SUPERPOSITION OF FORCED AND DIFFUSIVE FLOW IN A LARGE-PORE GRAPHITE

R. B. Evans, III, J. Truitt, and G. M. Watson

ABSTRACT

An experimental investigation of steady-state counter-flow of gases in a large pore graphite was carried out using an AGOT (National Carbon Co.) graphite septum exposed to sweep streams of helium and argon. The total pressures of the experiments ranged from 1.2 to 6 atmospheres; the temperatures were 24° to 27° and 100°C. The objectives of the investigation were to ascertain the mechanism of diffusion, verify flow equations applicable to the mechanism, and determine the parameters required to use the equations which describe the mechanism.

Forced flow experiments, from which permeability constants were obtained, revealed that Knudsen effects were small and that the turbulent flow region would be encountered at low flow rates. The results of uniform-pressure diffusion experiments, which led to a mutual-diffusion coefficient for the gas mixture, indicated that a normal diffusion mechanism was controlling and verified the existence of a net drift under these conditions. Comparisons of data from combined forced and diffusive flow experiments with predicted values demonstrated that reasonable estimates of the

combined flow could be made utilizing the data obtained in separate experiments.

INTRODUCTION

Design studies of high temperature gas-cooled reactors have shown the necessity of maintaining the gas coolant (helium) at the lowest possible levels of contamination with respect to radioactive fission products and corrosion promoting substances.[1,2] The introduction of rotating shafts[3] and other mechanical devices into the system as well as the possibility of fuel element container (or coating) failure pose contamination problems which cannot be solved by utilizing impermeable barrier materials. In such cases, it has been proposed to employ a coolant gas sweep stream which would oppose the tendency for undesirable vapors to enter the coolant system via diffusion.[4,5] Thus, considerable interest has been generated regarding the "back-diffusion" of gases such as water vapor, xenon and krypton against a stream of helium flowing through small cracks and porous materials.

The primary objective of this investigation was to gain some insight as to what the net and gross transport rates of the components of a binary gas mixture would be when the effects of diffusion and forced flow were combined; that is, when both concentration gradients and total pressure gradients were present.

Physically, the above conditions can be conveniently realized in systems composed of a porous septum which are swept by gases of different concentration and molar density at two exposed surfaces. Porous septum materials are convenient since they generally possess small channels in great numbers. This is important since forced volumetric flow rates are proportional to the average diameter raised to the fourth power whereas diffusion rates depend on lower powers of the average diameter. To attain relative rates which are measurable under a wide range of concentrations and pressures and under true steady state flow conditions, the use of a diffusion medium such as graphite or sintered metals is nearly essential.

The type flow system described above covers a large number of special cases with respect to the diffusion medium and the boundary conditions which might be imposed on the gases. This report is concerned with the interdiffusion rates of helium and argon within a permeable graphite at both uniform and non-uniform total gas pressure. The graphite selected for this investigation (National Carbon AGOT) was such that Knudsen permeability and diffusion effects would not be of importance. The mechanisms governing the transport would be common to most of the pores and applicable to a single capillary or tube. Steady state transport phenomena were the only type considered.

NOMENCLATURE

a	Permeability slip factor, $cm^2/dyne$ or atm^{-1}
A	Cross sectional area normal to flow, cm^2
B_0	Viscous flow permeability constant, cm^2
c	Particular velocity of a single molecule, cm/sec
$\overline{c^2}$	Mean square velocity, $(cm/sec)^2$
C	Concentration, $mole/cm^3$
d	Diameter of a circular conduit, cm
D_{12}	Mutual diffusion coefficient, cm^2/sec
D_0	Normalized mutual diffusion coefficient, cm^2/sec
D_i	Apparent diffusion coefficient, cm^2/sec
f_x	Force along x due to intermolecular collisions, dynes
h	Height of cylindrical graphite septum, cm
i	Subscript denoting a particular gaseous component
k	Permeability constant, darcy or cm^2
k_0	Permeability constant at infinite pressure, darcy or cm^2
$\overline{k}$	Boltzmann's constant, $1.3804 \cdot 10^{-16}$ $erg/^{o}K$-molecule
K	Permeability coefficient, cm^2/sec
K_0	Knudsen (slip flow) permeability constant, cm
L	Length along path of flow, cm
L_c/L	Tortuosity factor
m	Mass per atom or molecule, g
m^*	Reduced mass of an unlike pair of molecules, g

M	Molecular or atomic weight, g/mole
n	Total number of moles
$\dot{n}_f$	Forced-flow rate, mole/sec
$\dot{n}_i$	Total flow rate of component i, mole/sec
$\dot{n}_i'$	Diffusive flow rate at uniform pressure, mole/sec
$\dot{n}_T$	Net flow rate, mole/sec
$\underset{\sim}{\dot{n}}$	Flow rate as a vector, mole/sec
N'	Avogadro's number, $6.0247 \cdot 10^{23}$ molecule/mole
$N_i(x)$	Mole fraction of a component at a point x
P	Total pressure, dyne/cm^2 or atm
P_a	Pressure at which effluent Q_a is measured, dyne/cm^2 or atm
P_m	Mean flowing pressure, dyne/cm^2 or atm
Q	Volumetric flow rate, cm^3/sec
Q_a	Volumetric flow rate of effluent gas (generally at P_a = barometric pressure), cm^3/sec
r	Radius of cylindrical graphite septum (r_o = outer radius, r_i = inner radius), cm
R	Gas constant, 82.05 cm^3 atm/mole ^oK
Re	Reynold's number
T	Temperature, ^oK
t	Time, sec
$\bar{v}$	Mean thermal velocity, cm/sec
V	Total volume, cm^3

W	Weight fraction
x	Variable position along L, cm
x'	Particular position along L, cm
z	Radial thickness factor
β	Diffusive flow factor
δ_{12}	Total diffusive driving force, mole/cm^4
ΔP	Pressure drop along L, dyne/cm^2 or atm
ϵ	Open or connected porosity
ζ	Number of capillaries
η	Number of particles
μ	Fluid viscosity, dyne-sec/cm^2
ρ	Fluid mass density, g/cm^3
σ_{12}	Cross section for collisions of unlike molecules, cm
ϕ	Fraction of $\dot{n}_f$ acting on $\dot{n}_1'$

FUNDAMENTAL CONCEPTS

When consideration is given to a single or a group of parallel conduits (Knudsen effects absent) the ends of which are swept by gases of different composition, there will be a net flow of molecules under isothermal conditions even though the total pressure is uniform throughout the system. One would expect this with diffusion superimposed on forced flow; however, the fact[6,7,8] that a net flow will be present at uniform total pressure might not be immediately evident, particularly since the net flow is zero in the classical experiment. For this reason, a review of the classical diffusion experiment where the net molecular flow is always zero will be made before proceeding to a theoretical review applicable to the present investigation.

Mutual Diffusion

The Classical Experiment

The term mutual diffusion applies to the classical transient diffusion process which is employed to obtain diffusion coefficients for binary mixtures as tabulated in the literature. The diffusion medium is a long, vertical, equipartitioned tube. The pure component gases are introduced at the same pressure in the separate compartments with the heavier of the two in the lower compartment. At time, t_0, the partition is removed and

the concentration change of one of the gases, C_1, is followed as a function of time at a fixed position, x, or for a given volume fraction of the tube. An unsteady state mass balance combined with Fick's first diffusion law,

$$\dot{n}_1 = - D_{1\,2}\ A \frac{\partial C_1}{\partial x} , \qquad (1)$$

leads to the second Fick diffusion law,

$$\frac{\partial C_1}{\partial t} = D \frac{\partial^2 C_1}{\partial x^2} , \qquad (2)$$

which is applicable to the experiment. The symbol $\dot{n}_1$, is the molar flow rate, D is the coefficient to be determined, and A is the area of the tube normal to flow. Integration of equation (2) under appropriate boundary conditions leads to final equations which enable one to obtain D from the variables measured; that is, C_1, t, and x.

There are several interesting features of the diffusion process which can be readily discussed without tabulating the final integrated rate equations. The entire process is transient with time and the center of mass within the system shifts with respect to position since the concentrations of the components are not at equilibrium initially. No molecules are added to, or withdrawn from, the system during the process. The initially equal pressures in both compartments remain constant with time. There is no net molecular transfer with position. The individual

diffusion rates must be equal and opposite in direction; thus, the coefficients must be equal. During the process, the total momenta of the gases present are conserved.

A combination of experimental evidence and derivations appearing in several books covering the kinetic theory of gases has shown that standard mutual diffusion coefficients are independent of the composition of a given binary gas mixture and that the rates and coefficients depend only on the momentum exchanged between light and heavy components as a result of collisions of unlike molecules.[9,10] The derived relationship based on all conditions mentioned is

$$D_{12} = \left(\frac{3}{8}\right)\left(\frac{\pi \bar{k} T}{2m^*}\right)^{\frac{1}{2}}\left(\frac{V}{nN'\pi\sigma_{12}^2}\right), \qquad (3)$$

where N' is Avogadro's number and $\bar{k}$ is Boltzmann's constant.

Upon substitution of the perfect gas law,

$$PV = nN'\bar{k}T = nRT, \qquad (4)$$

one notes that the coefficient varies inversely with the square root of m* - the reduced mass,[a] with σ_{12}^2 - the collision diameter, squared and with P - the total gas pressure. The coefficient should vary directly with the absolute temperature raised

---

a. The reduced mass for a binary mixture is $m_1 m_2/(m_1 + m_2)$.

to the three halves power according to the simple theoretical derivation of equation (3). Very rigorous derivations and experimental evidence indicate that this power should vary from one binary mixture to another, for example the power is 1.75 for He-A mixtures and 1.74 for H_2-CO_2 mixtures at temperatures above 0^oC.[11]

If the driving force in Fick's first law is expressed as mole fraction N_1 per cm rather than C_1 per cm as in equation (1), it can be shown that the temperature and pressure dependencies of the coefficient and diffusion rates are quite different. The coefficient is inversely proportional to P; the rate is independent of P. Likewise, the coefficient is directly proportional to the temperature raised to some power around 1.5; the rates are proportional to some power near 0.5.

Transient Sweep Experiments

Another transient experiment similar to the foregoing involves a porous material which is initially saturated with one component at T and P - then swept along one face with a different gas at the same conditions. Although molecules are added to, and removed from, the system during this process, the net change is zero and the sweep gas serves to maintain one of the faces under a constant (or perhaps variable) known concentration with respect to the saturating gas. Here again, the diffusion rates

within the material would be equal and opposite in direction. The situation is drastically changed, however, when two different faces of the medium are swept by gases of different composition. The latter case, which corresponds to the experiments conducted during the present investigation, are discussed in the next section of the report.

Diffusion in Systems with Sources and Sinks

General Relationships

A schematic diagram of an isothermal diffusion system to which particles are continuously added and withdrawn during the diffusion process is shown in Figure 1(a). The shaded section represents a solid septum or partition which is traversed by channels of identical geometry. Pure gases, designated as 1 and 2, are swept past the channel openings at equal, or perhaps slightly unequal, pressures and at velocities which will maintain the diffused gas at negligible concentrations. A steady state equation which describes the relative rates at which gases 1 and 2 move through the channels is given by[2,6,12]

$$\dot{n}_1 = \dot{n}_T N_1 - D_{1\,2}\, A \frac{P}{RT} \frac{dN_1}{dx} \qquad (5a)$$

where $\dot{n}_1$ represents the flow rate (moles/sec) of gas 1, $\dot{n}_T$ is the net particle drift, and N_1 is the mole fraction of component 1. At any point x, the individual flow rate of gas 1 is the

UNCLASSIFIED
ORNL-LR-DWG 50582R

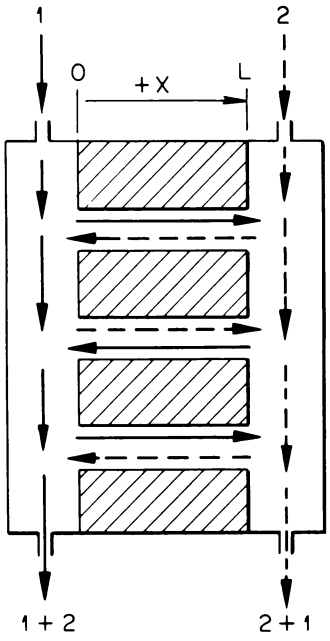

(a) DIFFUSION CELL

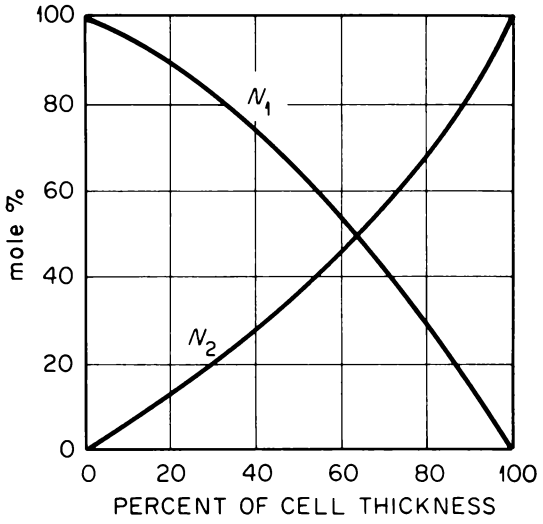

(b) CONCENTRATION PROFILES

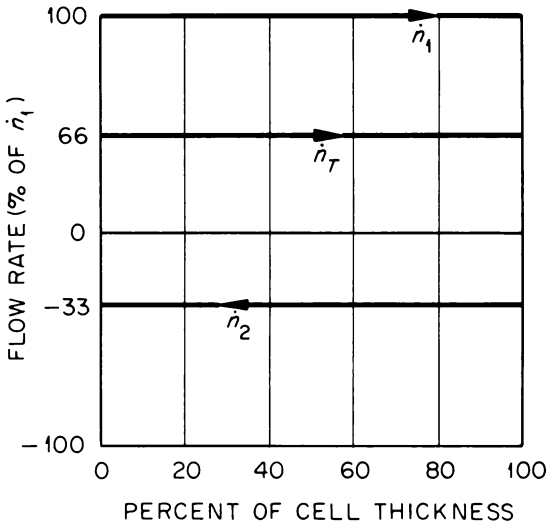

(c) NET FLOW RATES

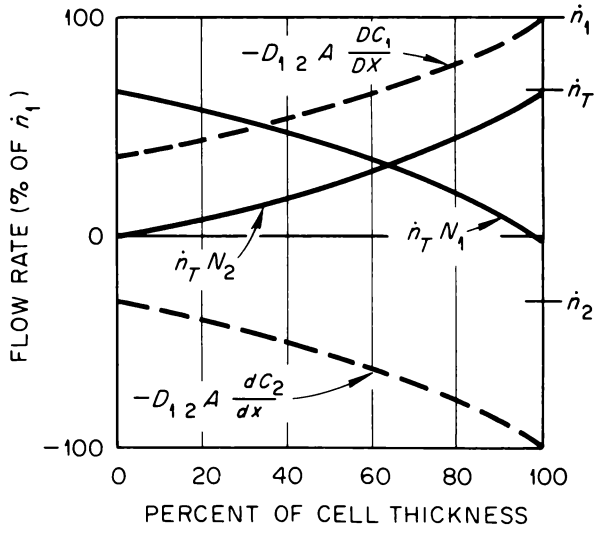

(d) FLOW RATE COMPONENTS

Fig. 1. Interdiffusion of Gases 1 and 2 with a Net Molecular Drift from 1 to 2.

sum of a mixed flow component and a Fick component. Although the value of each component varies along x, the sum of the components remains constant with position and time. Additional relationships which must hold are

$$\dot{n}_2 = \dot{n}_T N_2 - D_{21} A \frac{P}{RT} \frac{dN_2}{dx} , \tag{5b}$$

$$N_1 + N_2 = 1 , \tag{6}$$

$$D_{12} \frac{dN_1}{dx} = - D_{21} \frac{dN_2}{dx} , \tag{7}$$

as required by equations (3) and (6), and

$$\underset{\sim}{\dot{n}}_1 + \underset{\sim}{\dot{n}}_2 = \underset{\sim}{\dot{n}}_T \quad .^{b} \tag{8}$$

An integrated form of equation (5a) is

$$\dot{n}_T = D_{12} \frac{A}{x'} \frac{P}{RT} \ln \left[\frac{\dot{n}_1 - \dot{n}_T N_1 (x')}{\dot{n}_1 - \dot{n}_T N_1 (0)} \right] . \tag{9}$$

For additional discussion, it is convenient to consider a particular example where $\dot{n}_1 / \dot{n}_2$ is 3 under the boundary conditions mentioned, which are, $N_1 (0) = 1$, and $N_1 (L) = 0$. Equation (9) can be utilized to obtain the expression

$$(100) \frac{x}{L} \ln (3) = (100) \ln \left[\frac{\dot{n}_1 - \dot{n}_T N_1 (x)}{\dot{n}_2} \right] , \tag{10}$$

---

b. The positive x direction is taken as the direction of $\underset{\sim}{\dot{n}}_1$ (from left to right). Since $\underset{\sim}{\dot{n}}_2$ moves in the opposite direction, $\underset{\sim}{\dot{n}}_T$ is positive when $\dot{n}_1 > \tilde{n}_2$. The symbol $\underset{\sim}{\dot{n}}_1$ denotes a vector quantity; whereas, $\dot{n}_1$ is a scalar quantity representing $| \underset{\sim}{\dot{n}}_1 |$. Scalar notation is used in the discussion with the understanding that appropriate sign changes must be made in equation (9) when $\dot{n}_2 > \dot{n}_1$.

which gives the point concentrations as a function of the percent of the septum thickness. The assumed ratio $\dot{n}_1/\dot{n}_2$ and equation (8) require that $\dot{n}_2 = 0.333\dot{n}_1$ and $\dot{n}_T = 0.666\dot{n}_1$.

A plot showing the influence of a net drift $\dot{n}_T$ on the concentration profiles is presented in terms of the example stated on Figure 1(b). The relative magnitudes of rates $\dot{n}_1$, $\dot{n}_2$, and $\dot{n}_T$ are shown on Figure 1(c).

Figure 1(d), which shows the individual components as a function of percent thickness, graphically demonstrates the inter-relationships of the individual flow components. It is immediately apparent that the Fick components are symmetrical about a zero rate, and the mixed flow values are symmetrical about 0.5 $\dot{n}_T$. Following the mixed flow values (which add up at all points to give $\dot{n}_T$) from x/L = 0 to x/L = 100%, one may note that the net drift or sweep, $\dot{n}_T$, at x = 0 is composed of gas 1 - but exits as pure gas 2. This allows the Fick component of gas 1 to increase (along x/L) a corresponding amount such that all gas 1 exits as a Fick component at x/L = 100%. The gross rate of gas 2 entering at this point (as a Fick component) must equal the rate at which gas 1 exits. The former negative quantity and the positive gas 2 sweep component add up to yield the total transport rate $\dot{n}_2$. The only negative component present is the Fick component for gas 2.

It is also interesting to note how the curves would shift if $\dot{n}_T$ were forced to zero through a proper choice of experimental conditions. First, the concentration profiles would become linear and cross at x/L = 50%. The $\dot{n}_T$ of Figure 1(c) would disappear and $-\dot{n}_2$ would equal $\dot{n}_1$ and the mixed flow components would be zero. A knowledge of the causes of $\dot{n}_T$ is not required to show the manner in which $\dot{n}_1$ and $\dot{n}_2$ must vary with $\dot{n}_T$ or N_1 and N_2. This relationship is fixed by equation (9) as demonstrated on Figures 2 and 3. The curves of Figure 1 are based on point A, Figure 2; whereas, the curves of Figures 3, 4, and 5 are based on point B.

In review and for purposes of comparing the diffusion process of the classical experiment with that under discussion, it should be mentioned that the latter process is not transient with time, the center of mass of the system does not change with time or position, and the gases involved are not restricted to maintenance of a uniform total pressure. In the case of the mutual diffusion process the restrictions imposed required equal diffusion rates; such is not the case when sources and sinks are present. For the latter case, additional information as to the relative values of $\dot{n}_1$ and $\dot{n}_2$ is required to completely define the process. Equations (5a) and (5b) merely show the values the rates must assume in order to satisfy Fick's first

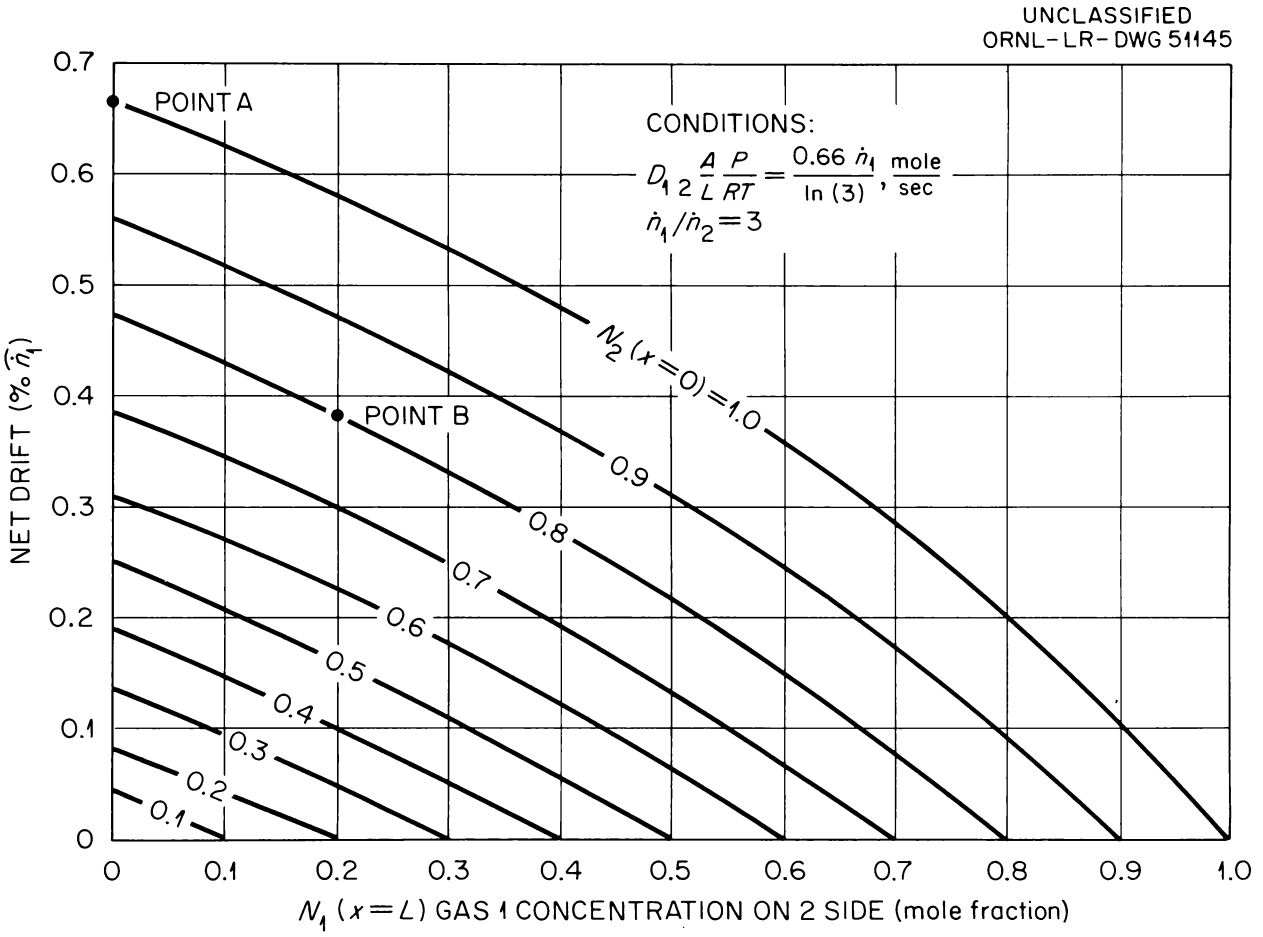

Fig. 2. Effect of Boundary Concentration on Net Drift at Uniform Total Pressure.

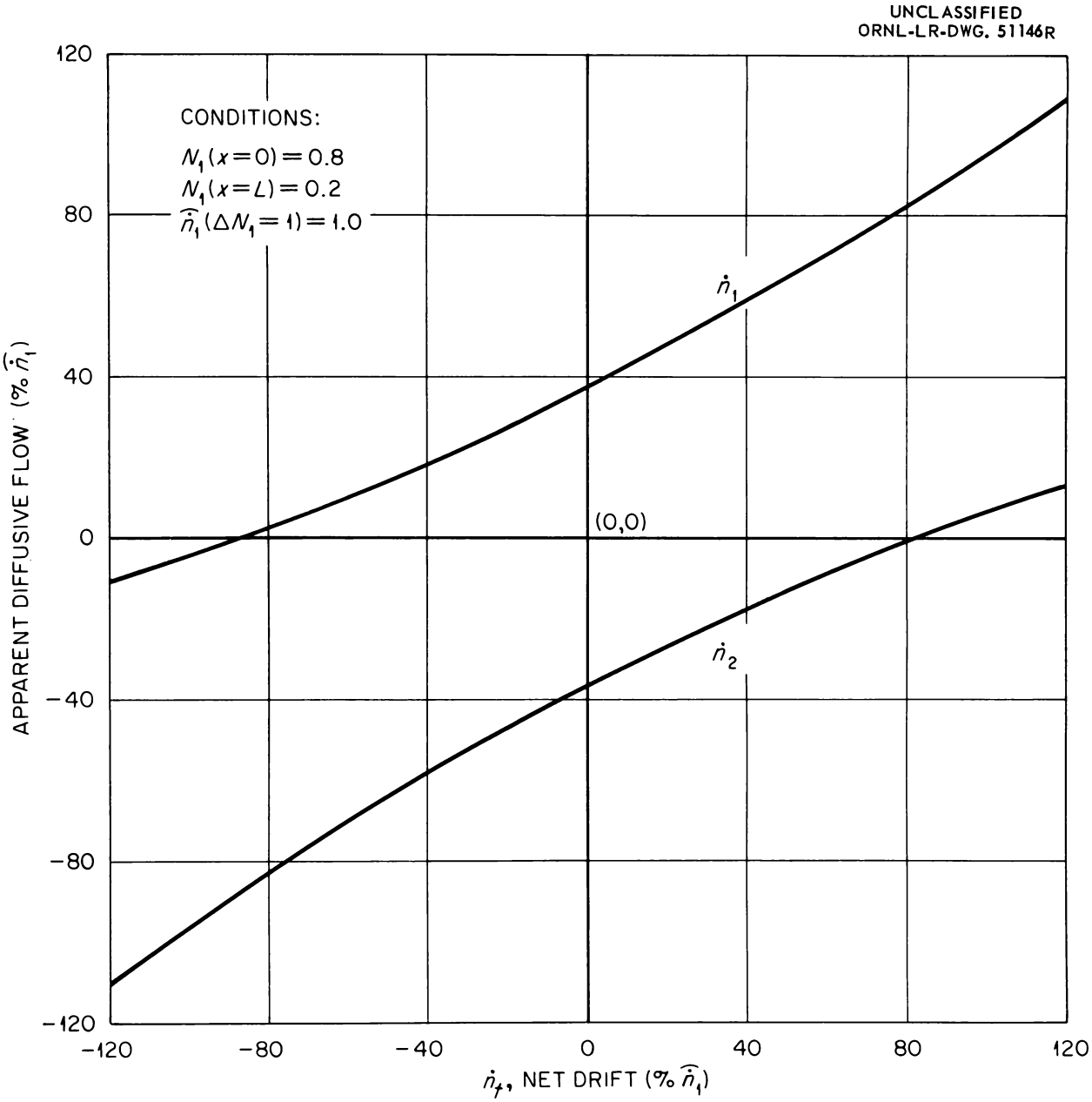

Fig. 3. Effect of Net Drift on Individual Transports.

diffusion law when a net drift is present. Factors which one must consider to predict the value of net drift or the $\dot{n}_1/\dot{n}_2$ ratio to be expected are discussed in the following sections.

Net Drift at Uniform Total Pressure

Uniform total pressure can be maintained on the gases contained in the apparatus of Figure 1(a) by proper adjustment of the sweep stream pressures. This operation can be performed with the aid of throttling valves and a sensitive manometer connected to the two sweep chambers. When the manometer liquid heights are the same, the gases in the system are at uniform total pressure - thus, the forces per unit area exerted on the liquid equal those exerted on the wall and those exerted on the gases contained in the channels of the septum.

One may recall a very elementary treatment of gas pressures and thermal velocities within a cube (L^3) whereby one considers the momentum change, 2mc, exerted on a wall when a single particle of mass m moving with a velocity c strikes the wall with a frequency c/2L. The force is mc^2/L. Extending this treatment to one third of the particles within the cube, that is, $\frac{\eta}{3}$ particles moving at a root mean square velocity of $(\overline{c^2})^{\frac{1}{2}}$ the total force on the wall becomes

$$m(\overline{c^2})^{\frac{1}{2}} - \left[-m(\overline{c^2})^{\frac{1}{2}}\right] \frac{(\overline{c^2})^{\frac{1}{2}}}{2L} \frac{\eta}{3} = P(L^2) \quad , \qquad (11a)$$

or

$$PV = \frac{1}{3}\,\eta\, m\, \overline{c^2} = \eta(\bar{k})\, T. \tag{11b}$$

By equation (11b) the root mean square velocity is:

$$(\overline{c^2})^{\frac{1}{2}} = \left(\frac{3RT}{M}\right)^{\frac{1}{2}}, \tag{12a}$$

which is nearly the same as the mean thermal velocity, $\bar{v}$, used in subsequent flow equations. The latter velocity is given by

$$\bar{v} = \left(\frac{8RT}{\pi M}\right)^{\frac{1}{2}}. \tag{12b}$$

Turning now to the diffusion experiments, it is clear that gas 1 passes through the channels at a steady rate $\dot{n}_1$, while gas 2 passes through in the opposite direction at a steady rate $\dot{n}_2$. The resulting net force exerted on all the gases between $x = 0$ and $x = L$ must be zero when the manometer indicates that a uniform pressure exists within the septum; that is,

$$\Sigma(f) = 0 = \dot{n}_1 N' \left[m_1 (\overline{c_1^2})^{\frac{1}{2}}\right] - \dot{n}_2 N' \left[m_2 (\overline{c_2^2})^{\frac{1}{2}}\right]. \tag{13}$$

Thus,

$$\dot{n}_1 / \dot{n}_2 = (M_2 / M_1)^{\frac{1}{2}}. \tag{14}$$

An equation for the net drift at uniform total pressure is then

$$\dot{n}_T = D_{1\,2}\, \frac{A}{L}\, \frac{P}{RT}\, \ln\left[\frac{1 - \beta N_1 (L)}{1 - \beta N_1 (0)}\right], \tag{15}$$

where

$$\beta = \left[1 - (M_1 / M_2)^{\frac{1}{2}}\right].$$

Net Drift at Non-Uniform Total Pressure

In the foregoing section, it was shown that one would expect higher rates of diffusion for the lighter components of a binary mixture than for the heavier components. Stated another way, one should expect the net drift to occur from the source of light gas toward the source of heavy gas even though the pressures at both sources are equal. It is pertinent to consider the effects of inducing or superimposing a forced flow on this system by means of a very small pressure drop. Under these conditions equations (5a) and (5b) should be

$$\dot{n}_1 = \dot{n}_T N_1 - D_{12} A \delta_{12}$$

and

$$\dot{n}_2 = \dot{n}_T N_2 - D_{21} A \delta_{21}$$

where δ_{12} is a driving force which replaces the dC_i/dx applicable at uniform total pressure.

The presence of a pressure drop within the system will alter the isothermal diffusion process in two ways; first, the net drift ($\dot{n}_T$) will be altered by the flow induced by the pressure drop; secondly, the driving force associated with D_{12} could be altered by a pressure diffusion term.

Pressure Diffusion

When the total pressure varies with position, one must consider the fact that the total diffusive driving force, δ_{12},

consists of two terms which are given by[2,13,14]

$$\delta_{1\,2} = \frac{\partial C_1}{\partial x} - W_1 \frac{\partial (n/V)}{\partial x} , \tag{16a}$$

where W_1 represents the weight fraction of gas 1. Since

$$\frac{\partial C_1}{\partial x} = \frac{P}{RT} \frac{\partial N_1}{\partial x} + \frac{N_1}{RT} \frac{\partial P}{\partial x} , \tag{16b}$$

$$\delta_{1\,2} = \frac{P}{RT} \frac{\partial N_1}{\partial x} + \frac{N_1 - W_1}{RT} \frac{\partial P}{\partial x} . \tag{16c}$$

The first term of equation (16c) is the familiar Fick first law-driving force; the second term is an expression for the "pressure diffusion" driving force which reflects the tendency for the heaviest molecules to migrate to high pressure regions within certain systems. To obtain some idea as to the relative magnitude of these terms, one may consider a case where: N_1 = 0.9 helium, N_2 = 0.1 argon, $\Delta N/\Delta(x/L)$ = 1, $\Delta P/\Delta(x/L)$ = 0.02 atm, and P_T = 2 atm. The ratio of the pressure diffusion term in equation (16c) to the concentration gradient term is less than 5×10^{-3} under these conditions. Similar calculations have shown that pressure diffusion effects can be ignored for practically all cases covered by the present investigation.

Forced Flow

When consideration is given to a diffusion system which is subjected to a pressure gradient which creates a forced flow,

it is general practice to consider the forced flow to be expected and then consider the diffusion as having been superimposed on the forced flow. Before going into a discussion of combining the forced flow and diffusive components, a very brief review of elementary forced flow behavior shall be presented.

The basic steady state relationship for forced flow in circular conduits is[15]

$$Q = \frac{\pi d^4}{128\mu} \cdot \frac{\Delta P}{L} = \frac{k}{\mu} \frac{A}{L} \Delta P \quad . \tag{17}$$

This equation is known as Poiseuille's volumetric flow formula for liquids. The symbol d represents the diameter of the circular conduit or capillary and k/μ is the ratio of permeability to liquid viscosity or the reciprocal of the resistance to flow. The derivation of this formula is based on the existence of a parabolic velocity profile within the capillary with a zero velocity at the walls. All of the external force $A \cdot \Delta P$ which causes the flow is transmitted to the tube wall through shearing stresses set up between the liquid laminae which move at different velocities. Equation (17) holds only in the viscous flow region.

To obtain a similar expression for gases in capillaries, it is necessary to combine the gas law (under specified thermodynamic conditions) with the volumetric law cited. For

isothermal conditions, one obtains

$$P_a Q_a = \dot{n}_f RT = \frac{k}{\mu} \frac{A}{L} P_m \Delta P \quad . \tag{18}$$

Equation (18) contains a base pressure, P_a, and a mean pressure, P_m, introduced via the gas law to take into account gas expansion along the pressure gradient.

As a result of the nature of the thermal agitation of gas particles (as compared to liquids), the velocity at the walls is not zero for gases in small capillaries. Thus equation (18) does not hold and deviations resulting from this apparent "slippage" along the walls is often greater than expansion effects. The constant k is actually $k_o(1 + \frac{a}{P_m})$ to take this into account. Under these conditions, another constant (actually a coefficient) is frequently employed. The definitive rate equation is

$$\dot{n}_f RT = K \frac{A}{L} \Delta P \quad , \tag{19}$$

where the coefficient is given by

$$K = K_o \frac{P_m}{\mu} + \frac{4}{3} \bar{v} B_o \quad . \tag{20}$$

It is interesting to note that the experimentally determined constant, k (cm^2), in equation (18) multiplied by P_m/μ gives the coefficient, K (cm^2/sec), and that this simple conversion automatically throws a single capillary equation (with slip)

into a parallel model consisting of two capillaries. One capillary is responsible for viscous effects; the other, for thermal velocity effects.

Superposition of Forced and Diffusive Flow Components

If a small pressure drop is maintained across a diffusion cell under conditions identical to those corresponding to point B, Figure 2, two relationships must be considered: First, equation (19) which involves the distribution of the external forces applied to the system; and, secondly, equations (5a) and (14) which govern the "internal" diffusion phenomena. The additional drift, $\dot{n}_f$, induced by the pressure drop is related to the final drift, $\dot{n}_T$, by the simple vector relationship,[9]

$$\underset{\sim}{\dot{n}}_T = \underset{\sim}{\dot{n}}_T' + \underset{\sim}{\dot{n}}_f \qquad (21)$$

where $\underset{\sim}{\dot{n}}_T'$ refers to the drift at uniform total pressure. The effect of varying $\dot{n}_T$ [through the use of equation (9)] is shown on Figure 3 which demonstrates that a change in the drift value alters both $\dot{n}_1$ and $\dot{n}_2$. This immediately suggests that equation (21) can be written as

$$\underset{\sim}{\dot{n}}_T = [\underset{\sim}{\dot{n}}_1' + \phi \underset{\sim}{n}_f] + [\underset{\sim}{n}_2' + (1-\phi)\underset{\sim}{n}_f] \qquad (22)$$

i.e., $\underset{\sim}{\dot{n}}_T = \underset{\sim}{\dot{n}}_1 + \underset{\sim}{\dot{n}}_2$, where ϕ represents the fraction of $\dot{n}_f$ acting on $\dot{n}_1'$.

The example of Figure 3 was then used to prepare plots of ϕ versus $\dot{n}_f$ [as dictated by equation (9)] shown on Figure 4. It is interesting to note that ϕ can be roughly approximated by a constant value of 1/2 within the $\dot{n}_f$ range of interest (+40 $\dot{n}_f$ to -120 $\dot{n}_f$, see Figure 5) and that the actual values tend to follow a straight line with the exception of regions near $\dot{n}_f = 0$. The physical significance of $\phi\dot{n}_f = 1/2\dot{n}_f$ is as follows: Superimposing a net flow of $\dot{n}_f$ on the system is equivalent to moving the entire cell (containing the uniform pressure drift) in the opposite direction through the sweep gases at a velocity equivalent to $1/2\dot{n}_f$.[c] The final $\dot{n}_1$ and $\dot{n}_2$ values refer to those crossing the cell boundaries under the new conditions of motion. It is clear that $\dot{n}_1'$, $\dot{n}_2'$ and $\dot{n}_T'$ appearing in equations (21) and (22) should be referred to the concentration boundaries applicable to the superposed case.

The interrelationships of all the flow components are presented on Figure 5. The dashed curves of $\dot{n}_1$ and $\dot{n}_2$ were obtained through the $\phi = 1/2$ approximation. Since $\dot{n}_T$ and $\dot{n}_f$ are related linearly, the curves of Figure 5 are merely those of Figure 3 shifted in such a way as to obtain the proper drift when $\dot{n}_f = 0$. The value of $\dot{n}_f$ may be obtained through equation (19) using an average K for the gas mixture. The relationships

---

c. It is clear that this is an approximation for $\dot{n}_f$ values near zero. At large positive $\dot{n}_f$ values, ϕ approaches 1, whereas ϕ approaches zero at large negative $\dot{n}_f$ values.

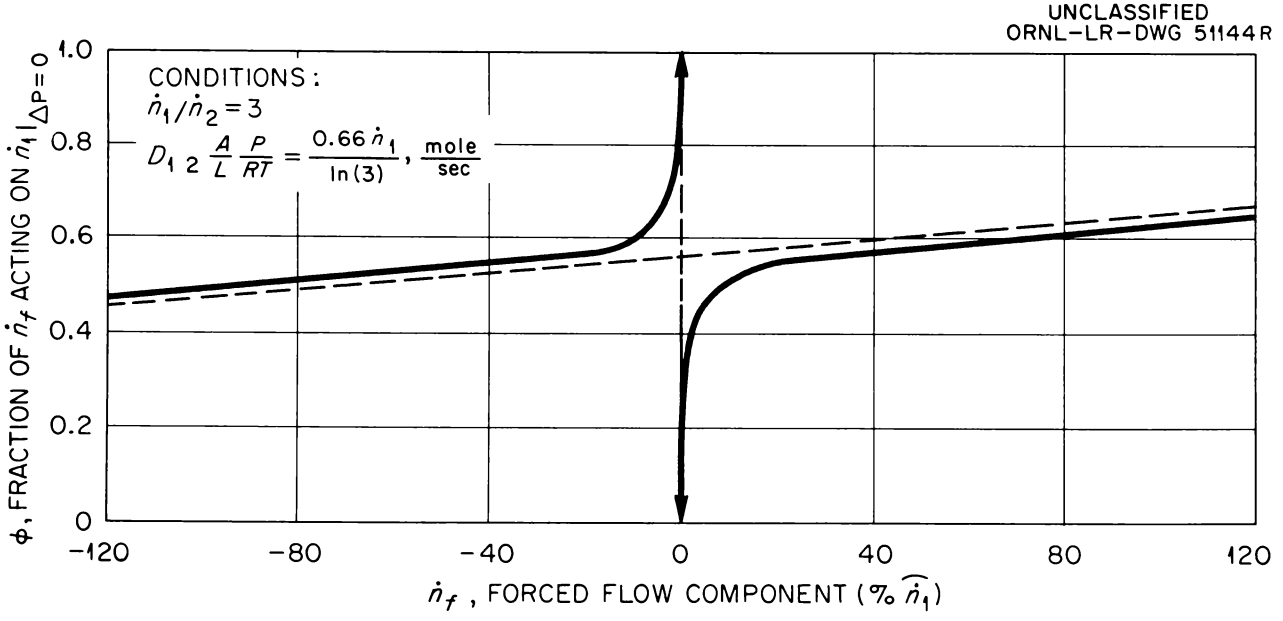

Fig. 4. ϕ vs n_f Relationship.

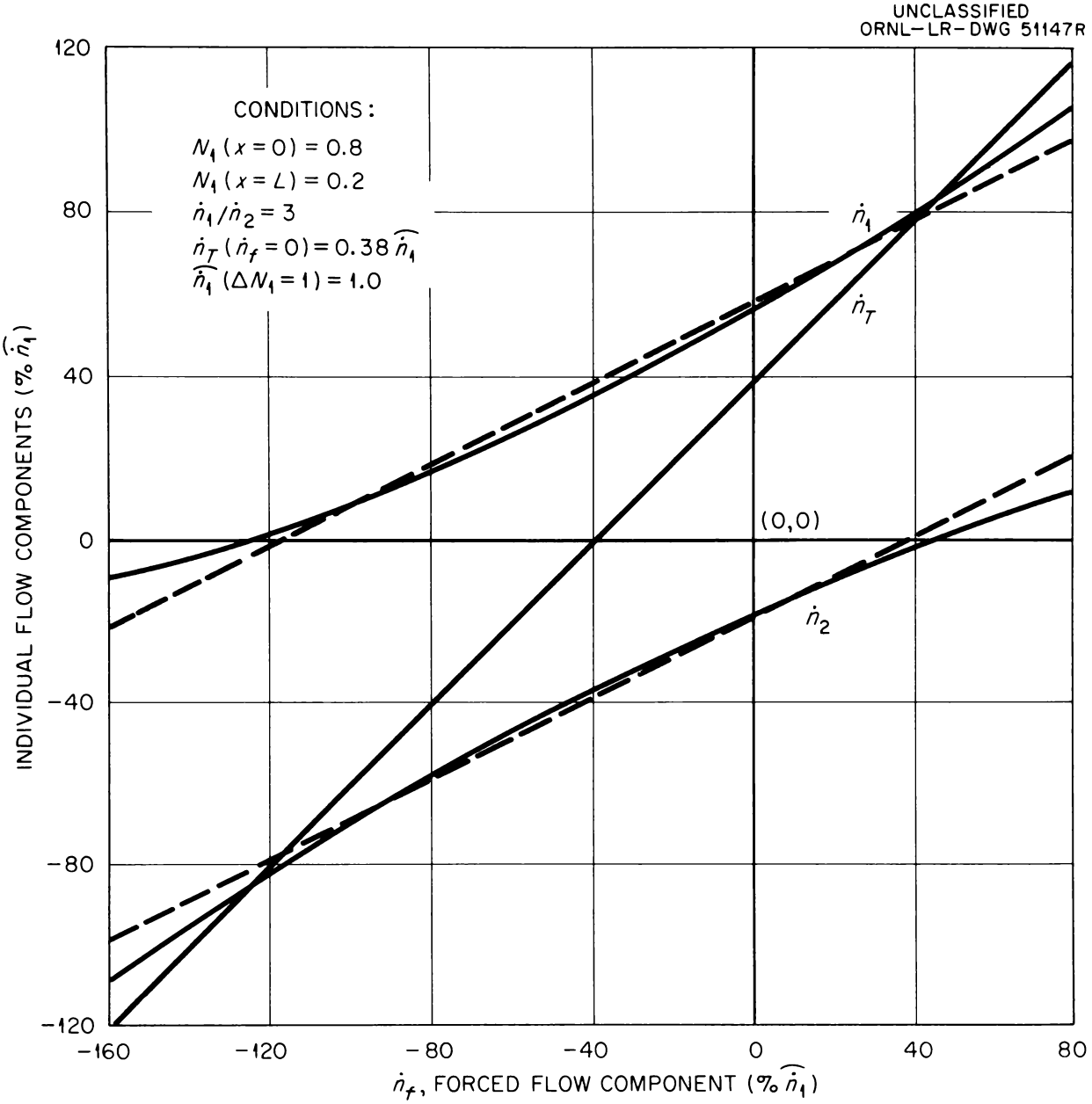

Fig. 5. Effect of Forced Flow on Individual Flow Components $\dot{n}_1$, $\dot{n}_2$ and $\dot{n}_T$.

between $N_1(x)$, $\dot{n}_1$, $\dot{n}_2$, $\dot{n}_T$, and $\dot{n}_f$ may be determined by equations (8), (9), (15), and (21). Equation (15) is used first to find $\dot{n}_T$ at $\Delta P = 0$, which with equations (8), (9), and (21), completely define the diffusion system.

Geometry of the Diffusion Medium

Up to this point discussions of the forced and diffusive flow phenomena have been made in terms of a model which consists of a group of parallel circular capillaries with equal "average" diameters. This is an oversimplification of the problem; however, use of this analogue enables one to discuss flow behavior in terms of established concepts without continually qualifying the parameters used with respect to the internal geometry of the medium.

Conversion of the model values to those of a porous material may be accomplished by equating free volumes and flow rates associated with each medium.[17] If the capillary bundle contains ζ channels and the porous material exhibits an open porosity ϵ, then $\zeta A_c L_c = \epsilon AL$ where the subscript c refers to a single capillary and no subscript means the gross value for a porous material. The rate equality is given by $\zeta(\dot{n}RT)_c = \dot{n}RT$, which is also given by the equation, $\zeta(D_c A_c/L_c) = DA/L$. Combining these equations, one obtains

$$D = \frac{\epsilon}{(L_c/L)^2} D_c \quad , \tag{23}$$

which may also be written terms of permeability constants. The L_c/L ratio is known as the tortuosity factor.

EXPERIMENTAL WORK

Diffusion Medium and Cell Arrangement

National Carbon Company AGOT graphite was selected as the diffusion medium since this material contains relatively large pores. The flow characteristics follow the mechanisms of interest and the rates involved are high enough to attain steady state diffusion conditions within one hour. Also, considerable data are available concerning the porosity,[18] pore size distribution,[19] permeability,[20] surface area,[21] and noble gas adsorption constants for AGOT graphite.[21]

The diffusion septum was prepared in the form of a thin walled cylinder. The exposed length was 4 in., the outer diameter was 0.8 in., and the inner diameter was 0.5 in. This gave an A/L ratio of 135.8 cm using the radial flow formula for steady state flow.[d] A photograph of the diffusion cell assembly

---

d. The area to length ratio is: $\frac{A}{L} = \frac{2\pi h}{\ln \frac{r_o}{r_i}}$.

This relationship is applicable to either forced or diffusive flow in a radial system.

is presented as Figure 6. The components, from left to right, are: the argon outlet which contains the thermocouple wires, the container, the diffusion septum and container cap, and the inner helium flow guide. For a diffusion experiment, helium was admitted through the upper tee. The helium moved down the 1/4 to 1/8 in. tubing annulus around the outside of the flow guide (sweeping the inner face of the graphite) and back up the inside of the guide and 1/8 in. tubing. Argon was admitted to the lower tee where it moved down the tee wall to 1/4 in. tubing annulus, then around the outer face of the graphite. The effluent argon left via the bottom of the container. During a permeability determination (forced flow experiment) of the septum, the side arm of the lower tee was plugged. The test gas was admitted at the bottom, forced through the graphite and out both the 1/4 to 1/8 in. tubing annulus and the 1/8 in. tubing proper which were connected in parallel. This was done to minimize the pressure drop through the apparatus.

It was necessary to conduct forced flow experiments with the diffusion cell after it was completely assembled in order to determine the integrity of the graphite to metal seals, to verify that Knudsen effects would be small, and to obtain permeability data for subsequent diffusion experiments.

UNCLASSIFIED
PHOTO 36002

Fig. 6. Diffusion Cell and Graphite Septum.

Forced Flow Experiments

Experimental Procedures

A review of the various techniques employed in the laboratory for conducting forced flow experiments has been presented in detail in previous reports[18,20] and the open literature.[22,23,24] These methods are by no means original and may be classified as routine determinations. Briefly, the variables appearing in equation (18) were carefully measured with appropriate devices. The effluent flow rate Q_a was measured at P_a utilizing a calibrated wet test meter and a barometer. The pressure drop ΔP was measured directly with a manometer containing either butyl phthalate or mercury; the mean pressure was measured with calibrated Bourdon gages. The A/L ratio was known as well as the gas viscosities at various temperatures.

Results and Discussion

The first experiments involved the determination of the maximum flow rate or $P_m \cdot \Delta P$ product which would demonstrate viscous flow behavior since the flow must be in the viscous region to evaluate permeability constants. Transition from viscous to turbulent flow occurs relatively abruptly in carefully

conducted pipe experiments at Reynolds numbers[e] around 2000. In porous materials, the velocities at which transition occurs are much lower than in pipes[25] and must be determined experimentally. The results of this experiment are shown on Figure 7. The only linear curve on Figure 7 is that for helium at Q_aP_a values less than 125 cm^3-atm/sec at 20°C. Using Reynolds numbers calculations, the corresponding value for argon is 14.3 cm^3-atm sec. All other data on this figure correspond to measurements conducted in either the turbulent or the transition regions.

Permeability data for helium and argon are shown on Figures 8 and 9 which are conventional plots for equations (18) and (19). Contributions resulting from Knudsen effects are reflected by the slope of Figure 8 curves and the intercepts of the Figure 9 curves. Smoothed data corresponding to Figure 9 are shown in Table I. These results were correlated on the basis of viscosity data[26,27] for pure argon and helium which are reproduced in Table II.

---

e. The Reynolds number is given by $Re = 4Q\rho/\pi\mu d$ where ρ is the fluid mass density. One may think of this number as being a dimensionless velocity. In the viscous flow region, the velocity versus pressure drop relationship (Darcy's law) does not include a fluid mass density term. This factor enters the flow relationship when the flow is turbulent.

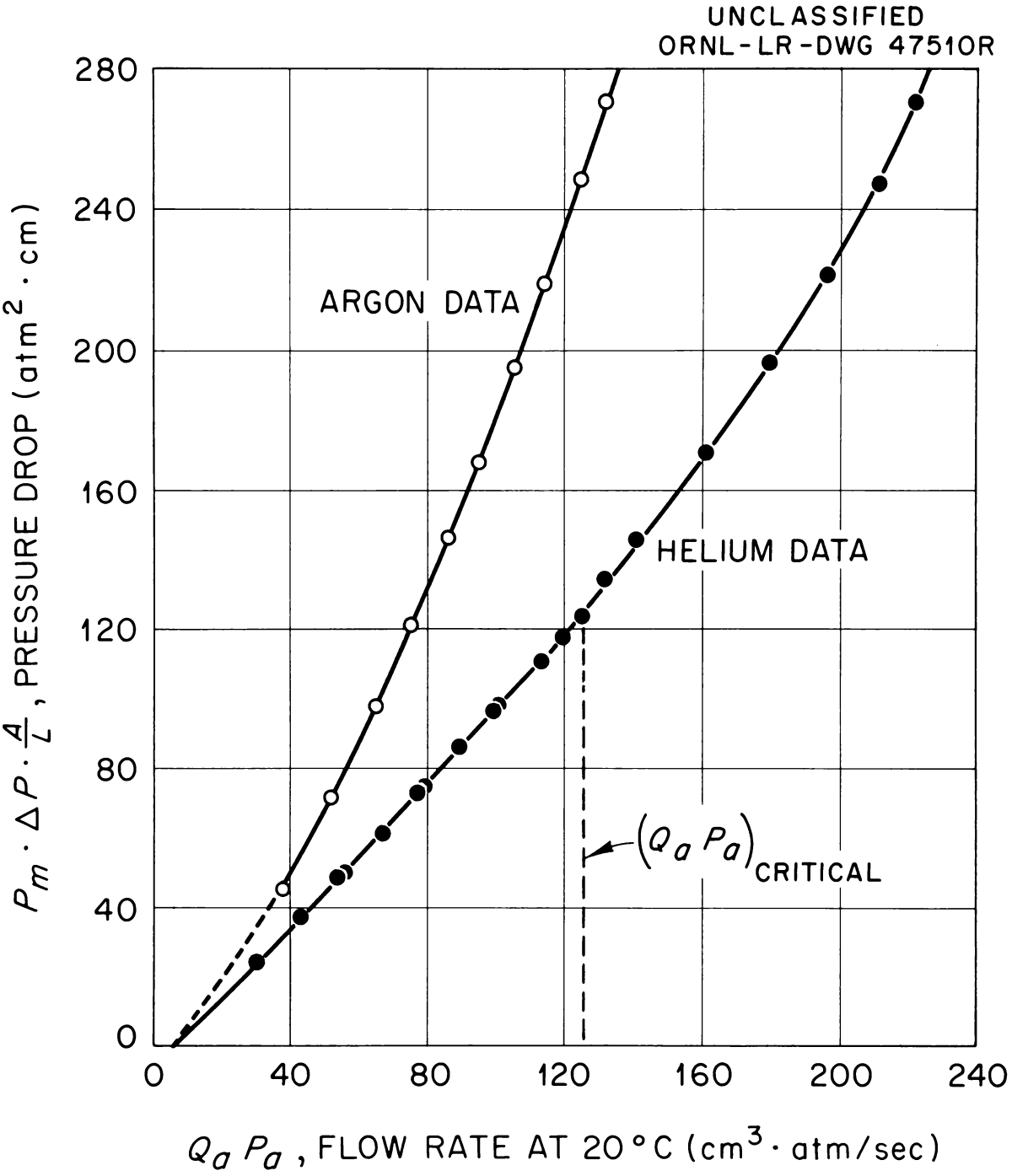

Fig. 7. Viscous and Turbulent Forced Flow Characteristics of Diffusion Septum at 20°C.

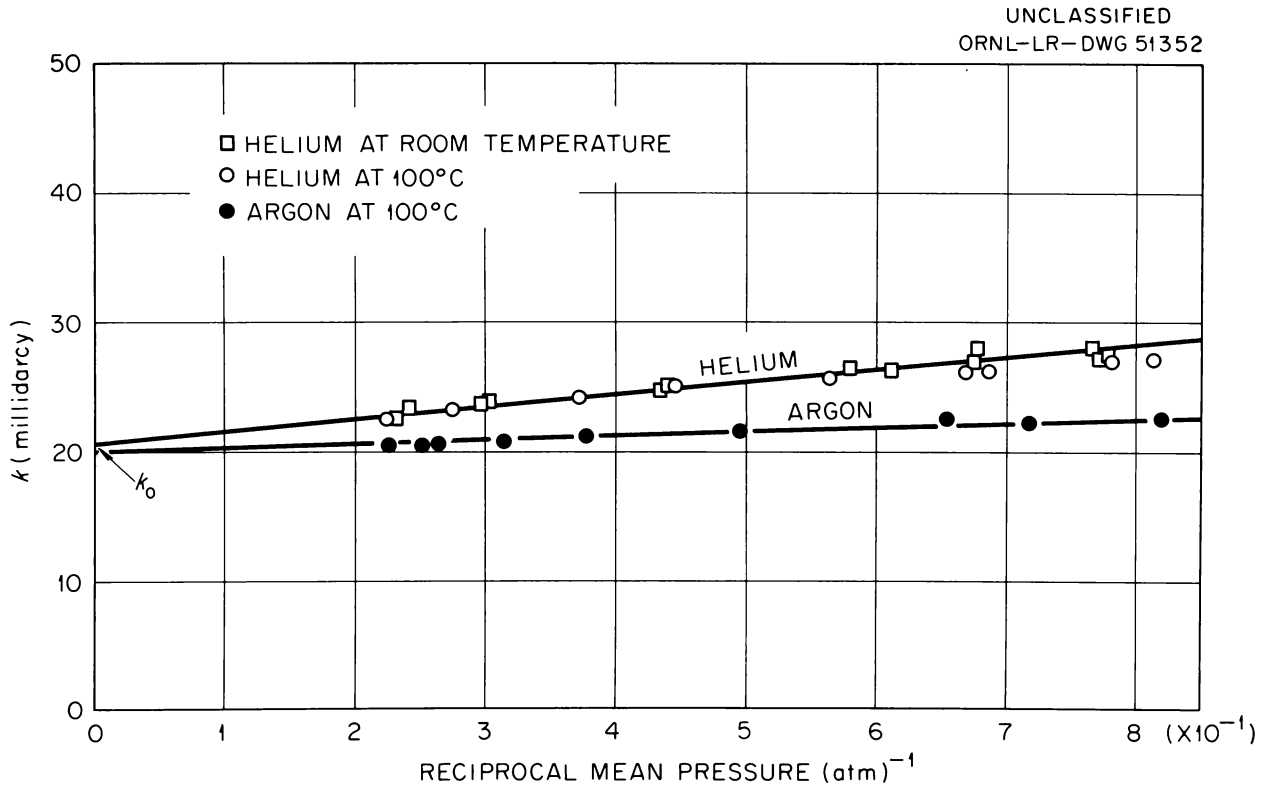

Fig. 8. Generalized Permeability Constants for Diffusion Septum.

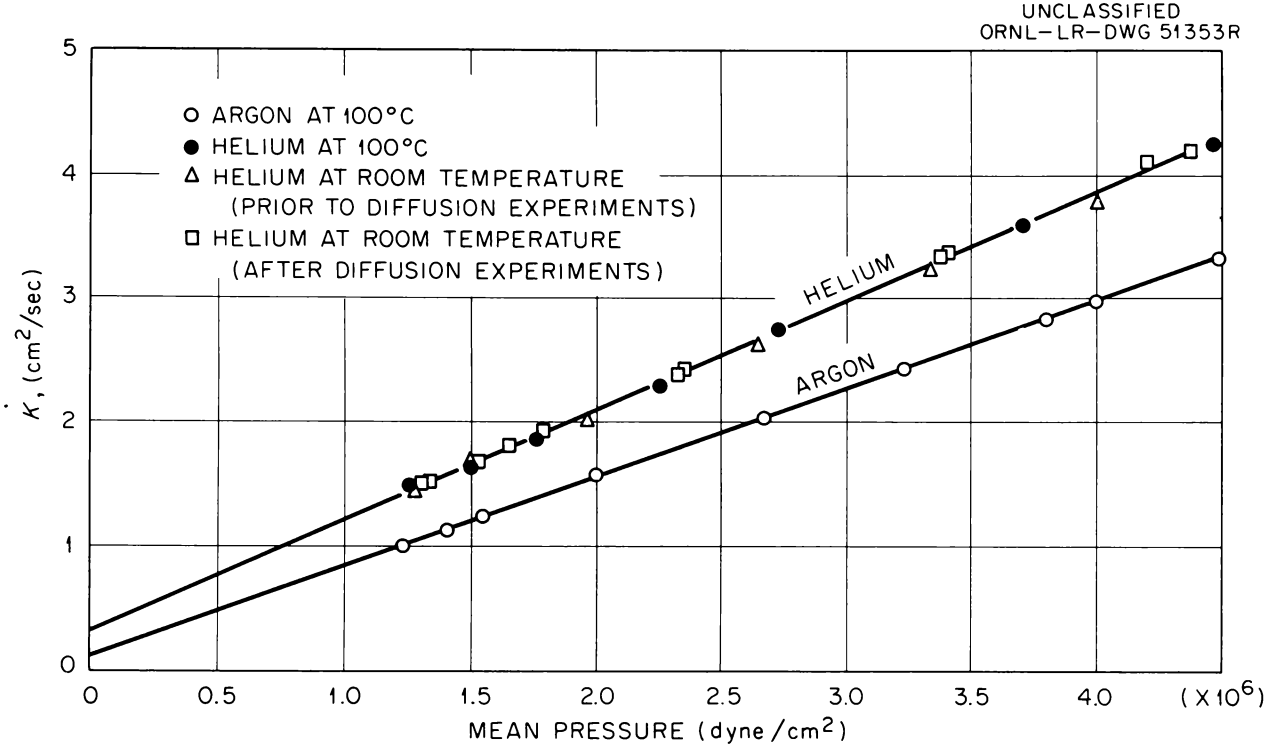

Fig.9. Individual Permeability Constants for Diffusion Septum.
(all values normalized to 100° C)

Table I. Smoothed Permeability Values Obtained from Figure 9

Mean Pressure (atm)	Permeability, K (cm^2/sec)			
	Helium		Argon	
	20°C	100°C	20°C	100°C
0	0.11	0.10	0.41	0.36
1	0.94	0.82	1.40	1.24
2	1.75	1.55	2.38	2.12
3	2.58	2.29	3.36	2.97
4	3.41	3.02	4.35	3.86
5	4.24	3.76	5.36	4.75
6	5.06	4.49	6.36	5.64

Table II. Viscosity of Pure Helium and Argon Used for Correlating Permeability Data

Temperature (°C)	Viscosity (poise)	
	Helium[a]	Argon[b]
	x 10^{-4}	x 10^{-4}
20	1.95	2.22
40	2.04	2.34
60	2.13	2.46
80	2.22	2.57
100	2.31	2.68

a. H. L. Johnson (ref 26).

b. J. O. Hirschfelder et al., (ref 12).

The permeability of the septum to various helium-argon mixtures was of particular interest as this information was required to draw comparisons between predicted and experimental results for the superposed flow experiments. The mixture values at the conditions of interest (1.96 atm, 100°C) were estimated using permeability data for the pure gases and published viscosities of helium-argon mixtures.[28] It was assumed that the intercept as given by equation (20) varied linearly with composition. The viscosity ratios were used to correlate the viscous flow terms. The results of the permeability estimations and viscosities at 100°C and 1.96 atm are shown below as a function of helium content.

Mole fraction helium	0.20	0.40	0.60	0.80
Viscosity, poise	2.75	2.81	2.83	2.75×10^{-4}
Estimated K, cm^2/sec	1.56	1.58	1.63	1.72

The next step involved averaging the above values to take into account the large concentration variation present within the pore (resulting from back diffusion) during a superposed experiment. This will be discussed in the section which covers superposed flow.

Diffusion Experiments

Experimental Procedures

The complete hook-up of the cell and auxiliary lines for the diffusion experiments is shown on Figure 10. Argon and helium were admitted at the non-bleed regulators, passed through the sweep chambers of the cell, and throttled at atmospheric pressure at the needle valves. The throttled gas was passed through a wet test meter to measure the sweep rates. These data combined with the results of analyses of gas samples taken at points A and A' (see Figure 10) led to the rates of diffusion or forced flow through the graphite. Both uniform pressure and superposed experiments were carried out with this apparatus. The amount of pressure drop across the septum was determined by means of the manometer which contained butyl phthalate. For the 100°C experiments, the diffusion cell and preheating lines were submerged in a container which contained eighteen gallons of thermostated oil.

Prior to the diffusion experiments, a series of carefully conducted calibrations was made to determine the pressure drop (at various sweep rates) between the manometer taps and the first point of exposed graphite. From this point on the pressure drop per unit length of graphite within the cell was the same on each side when the sweep rate of each gas was the

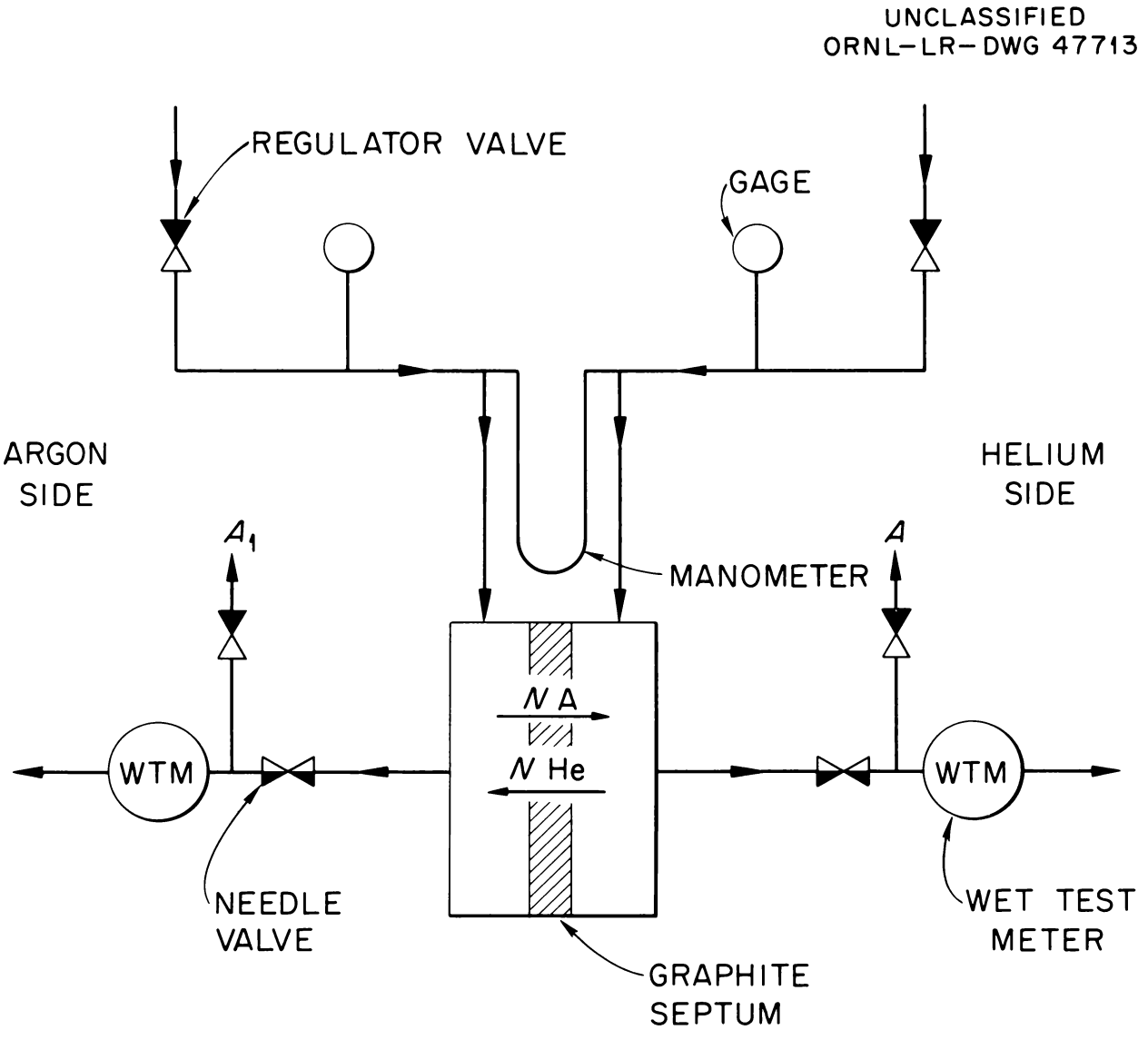

Fig. 10. Line Drawing of Diffusion Apparatus.

same. However, it was necessary to apply a slightly higher pressure on the helium inlet than on the argon inlet to obtain equal pressures on both sides of the septum as the inlet line drops were not equal.

All flow meters, thermometers, and Bourdon gages were calibrated through suitable standards and procedures. The gases were analyzed by mass spectrometric methods. In many cases, steady-state flow conditions were established through the use of thermal conductivity cells placed in parallel with the wet test meters. The estimated maximum error to be expected in a single determination of the coefficient was ± 5%. As it turned out, the average deviation of thirty-two determinations of the coefficient was ± 3%. Only three experiments had a deviation from the average greater than 5%.

The apparatus and procedures used in this investigation were originated by Wicke[29,30] as a means of studying surface diffusion. Although Wicke subsequently turned to other procedures[31,32] to carry out surface diffusion studies, his original method has been employed by Wheeler,[32] Weitz,[33] Walker[34] and Hoogschagen[7] for diffusion studies involving porous media and binary mixtures. It appears that Hoogschagen[7] was the first to analyze both sweep streams; that is, measure the diffusion rates of both gases present. However, the authors

have been informed through a recent personal contact that Wicke is now conducting experiments where both streams are analyzed.

Results and Discussion of Uniform Pressure Experiments

Two sets of uniform pressure experiments were performed; one at room temperatures (24^{o} to $27^{o}C$), and another at $100^{o}C$. In addition, a third set was performed at $100^{o}C$ wherein the pressures on each side of the septum were slightly unbalanced. The results of these experiments are presented and discussed in the light of the various objectives which suggested the experiments.

Apparent Coefficients and Knudsen Effects.--If one assumes that the individual diffusion rates can be approximated by the equation

$$\dot{n}_A = D_A \frac{A}{L} \frac{P}{RT} \Delta N_A \quad , \tag{24}$$

it is possible to define a coefficient in terms of a Knudsen resistance and a normal resistance. The combined coefficient for argon (actually, the measured or effective coefficient) would be given by the relationship

$$\frac{1}{D_{eff,A}} = \frac{1}{D_{N,A}} + \frac{1}{D_{K,A}} \quad , \tag{25}$$

where $D_{N,A}$ is the apparent normal-diffusion coefficient, which

depends on intermolecular collisions, and $D_{K,A}$ is the Knudsen coefficient, which depends on collisions with the pore walls. Equation (25) results from a series resistance model and the fact that equation (24) is the definitive rate equation for both pure Knudsen and normal diffusion processes when the concentration profiles are linear. To estimate the contribution of each mechanism one must examine the manner in which $(D_{eff,A})^{-1}$ varies with either pressure or temperature. For example, a plot of reciprocal coefficients obtained at a single temperature and various pressures should be a horizontal line with respect to pressure if the mechanism is pure Knudsen flow, a straight line with a positive slope going through the origin if the mechanism is normal diffusion, and finally a straight line with an appreciable intercept if a combined mechanism exists.

A plot of the uniform pressure data correlated according to equations (24) and (25) is shown on Figure 11. The small intercept values indicate that Knudsen effects are small and the straight lines verify the primary role of the normal diffusion. Thus the diffusion mechanism under study depended entirely on intermolecular collisions, not on wall collisions. The only contribution of the AGOT graphite was with respect to the magnitude of the rates and coefficients measured. This

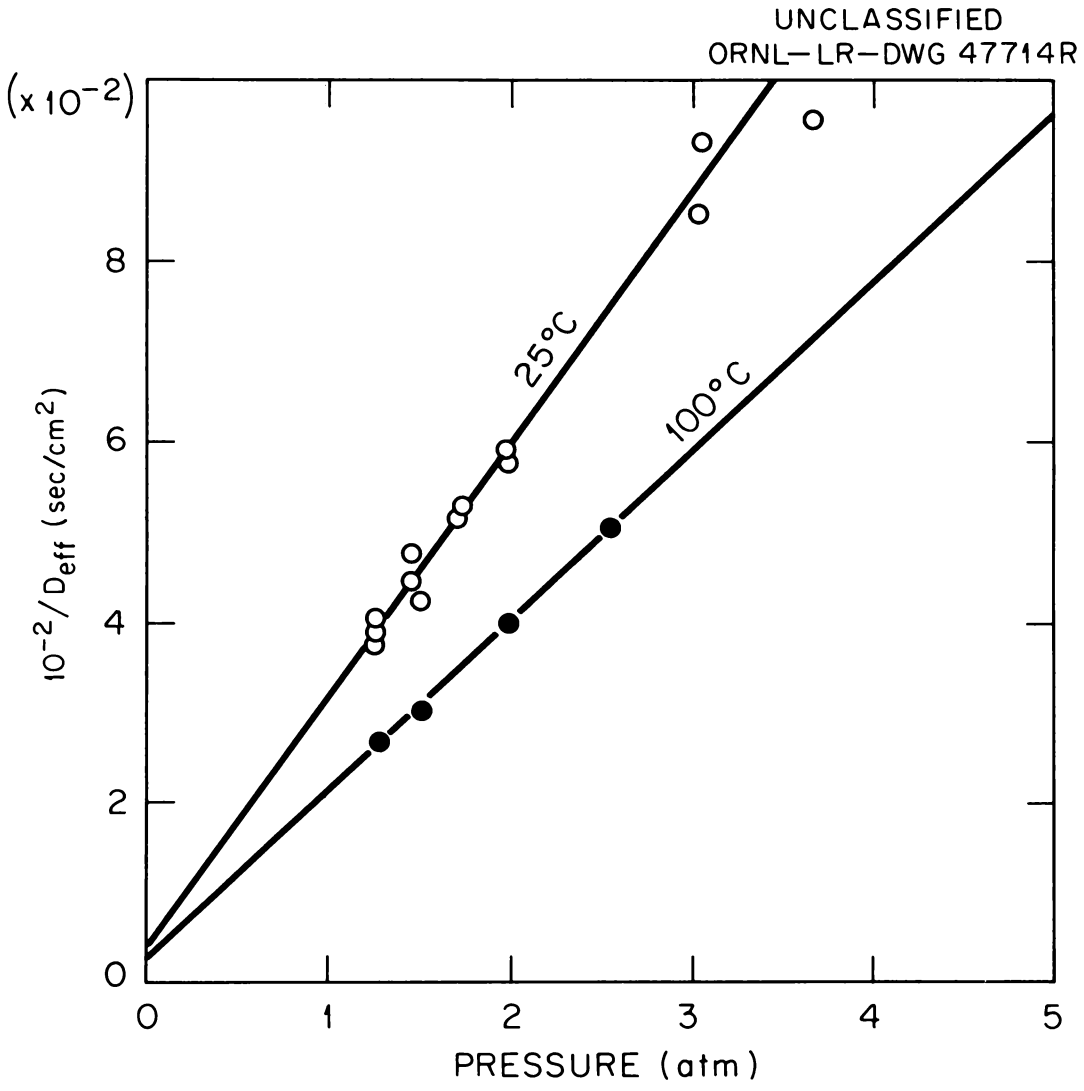

Fig. 11. Reciprocal Apparent Diffusion Coefficients for Argon Versus the Uniform Total Pressure of the Experiment.

material had no effects on the mechanisms of diffusion at the pressures, temperatures and sweep rates of the experiments.

Net Drift at Uniform Pressure.--Diffusion rate results for the uniform pressure experiments have been tabulated in Tables III and IV. These data required no correlation in that they result from the effluent sweep rates and the gas analyses. The point under discussion is demonstrated by the columns denoted $\dot{n}_{He}$, $\dot{n}_A$, $\dot{n}_T$ and, in particular, the $\dot{n}_{He}/\dot{n}_A$ ratio. In every case $\dot{n}_{He} > \dot{n}_A$. Furthermore, the experimental ratio, $\dot{n}_{He}/\dot{n}_A$ remained the same (within the precision with which pressure uniformity could be maintained) regardless of the temperature and pressure of the experiment. The average ratio for the eighteen experiments of Tables II and III was 3.28. The difference between the above value and the theoretical value (3.16) was 3.8% of the latter. However, this was less than the uncertainty associated with the manometer reading and calibration data which amounted to ± 7% of the correct value as based on permeability data.

Additional data regarding this ratio for other binary mixtures in a large pore graphite subjected to Wicke's boundary conditions have been reported by Hoogschagen.[7] These values are reproduced below for the reader's convenience.

Table III. Results of Uniform Pressure Experiments Conducted at Room Temperature

Temperature T (°K)	Pressure P (atm)	Mole Fraction of Helium at x=0	Mole Fraction of Helium at x=L	Diffusion Rates (mole/sec) $\dot{n}_{He}$	Diffusion Rates (mole/sec) $\dot{n}_{A}$	Diffusion Rates (mole/sec) $\dot{n}_{T}$	Ratio of Helium to Argon Diffusion Rate	Diffusion Coefficient[a] D_{12} (cm²/sec)
				$x10^{-5}$	$x10^{-5}$	$x10^{-5}$		$x10^{-3}$
299.7	1.249	0.9935	0.0232	6.07	1.72	4.35	3.53	6.17
298.4	1.251	0.9866	0.0446	5.75	1.73	4.02	3.32	6.17
297.1	1.251	0.9867	0.0439	5.66	1.71	3.94	3.31	6.11
301.1	1.475	0.9874	0.0454	5.78	1.61	4.17	3.59	5.97
299.3	1.475	0.9862	0.0434	5.52	1.77	3.75	3.12	6.06
300.5	1.500	0.9947	0.0169	6.18	1.94	4.24	3.19	6.47
298.7	1.740	0.9962	0.0132	6.14	1.80	4.34	3.41	6.28
295.7	1.740	0.9863	0.0419	5.45	1.79	3.66	3.04	6.07
295.4	1.975	0.9862	0.0440	5.69	1.80	3.90	3.16	6.28
297.3	1.992	0.9958	0.0132	6.03	1.92	4.11	3.14	6.40
298.7	3.005	0.9872	0.0442	5.79	1.70	4.09	3.41	6.11
300.5	3.005	0.9861	0.0421	5.49	1.84	3.64	2.98	6.14
298.1	3.704	0.9950	0.0146	6.18	2.13	4.05	2.90	6.76
298.2	6.351	0.9857	0.0358	6.35	1.64	4.71	3.87	6.42

a Normalized to 20°C and 1 atm by the relationship $D=D_0\left(\frac{P_0}{P}\right)\left(\frac{T}{T_0}\right)^{1.75}$.

Table IV. Results of Uniform Pressure Experiments Conducted at 100°C

Pressure P (atm)	Mole Fraction of Helium		Diffusion Rates (mole/sec)			Ratio of Helium to Argon Diffusion Rate	Diffusion Coefficient[a] D_{12} (cm^2/sec)
	at x=0	at x=L	$\dot{n}_{He}$	$\dot{n}_A$	$\dot{n}_T$		
			$x10^{-5}$	$x10^{-5}$	$x10^{-5}$		$x10^{-3}$
1.25	0.9851	0.0485	6.30	1.95	4.35	3.23	5.80
1.48	0.9846	0.0507	6.50	2.00	4.51	3.25	6.10
1.96	0.9844	0.0508	6.63	2.02	4.61	3.29	6.09
2.51	0.9842	0.0532	6.93	2.05	4.88	3.39	6.31

Table V. Results of 100°C Experiments Conducted with $P_A - P_H$ = 1.43 mmHg at Various Total Pressures

Pressure P (atm)	Mole Fraction of Helium		Diffusion Rates (mole/sec)			Ratio of Helium to Argon Diffusion Rate	Diffusion Coefficient[a] D_{12} (cm^2/sec)
	at x=0	at x=L	$\dot{n}_{He}$	$\dot{n}_A$	$\dot{n}_T$		
			$x10^{-5}$	$x10^{-5}$	$x10^{-5}$		$x10^{-3}$
1.98	0.9834	0.0375	5.89	2.51	3.38	2.34	6.49
1.51	0.9789	0.0489	5.78	2.36	3.42	2.45	6.48
1.27	0.9829	0.0423	5.77	2.30	3.47	2.51	5.91
2.97	0.9783	0.0397	5.59	2.90	2.69	1.93	6.46

a Normalized to 20°C and 1 atm by the relationship $D=D_0\left(\frac{P_0}{P}\right)\left(\frac{T}{T_0}\right)^{1.75}$.

Gases (1 - 2)	Average Ratio (Experimental)	Theoretical Ratio $(M_2/M_1)^{\frac{1}{2}}$
He - O_2	2.73 (3 determinations)	2.83
N_2 - O_2	1.08 (2 determinations)	1.07
CO_2 - O_2	0.845 (2 determinations)	0.85

The results of the present investigation coupled with those of Hoogschagen demonstrate that equation (14) is correct. This equation holds regardless of the obvious lack of rigor inherent in equations (11) through (13).

Mutual Diffusion Coefficients.--Having established the absence of Knudsen effects and the presence of a net drift, the next step consisted of calculating the individual coefficients utilizing the equations set forth by Present[9] and Hirschfelder.[12] As the reader may recall, the equations led to equations (9) and (15); the former was employed to express the measured rates and the average sweep concentration in terms of the mutual diffusion coefficient for helium-argon mixtures in the particular graphite investigated. The calculated coefficients at all the experimental temperatures and pressures were then normalized to 20°C and 1 atmosphere according to the

Lonius equation[11]

$$D = D_0 \left(\frac{P_0}{P}\right)\left(\frac{T}{T_0}\right)^{1.75} \qquad (26)$$

where D_0 is the normalized value. The coefficients resulting from the uniform pressure experiments are shown in the last column of Tables III and IV.

Non-Uniform Pressure Coefficients.--These were the first experiments conducted under superposed flow conditions. A small ΔP was maintained across the septum at four different mean pressures. The results are shown in Table V. Although the ΔP altered the individual rates considerably, the coefficients are essentially the same as those obtained under uniform pressure conditions. Thus it is not necessary to maintain a uniform total pressure within the cell during an experiment in order to determine the correct coefficient. The pressure drop present must be small (to avoid compression effects) and constant with time. The average coefficient for all the experiments of Tables III, IV, and V was 6.23×10^{-3} cm^2/sec.

Porosity and Tortuosity Factor.--Having obtained the overall diffusion coefficient for one binary mixture in this particular graphite, it would be most desirable to predict coefficients for other mixtures applicable to the same graphite.

This can be done by means of equation (23), which relates the free-space coefficient to the over-all coefficient through the ratio of the open porosity to the tortuosity factor.

In addition to the above application, the open porosity is also required to perform estimates of transient diffusion or forced flow rates since the gas can be accumulated or depleted only in the open pores of the graphite.

The open porosity of a sample of the same material used for the septum was determined by a helium saturation technique.[35] This value was 22.0 vol. %. The free space coefficient for helium-argon mixtures is 0.726 cm^2/sec at 20°C and 1 atmosphere. The above values combined with the over-all value reported for the septum at the same conditions resulted in a tortuosity factor of 5.07. Similar values utilizing permeability data are discussed by Carman[36] and Hutcheon.[17]

Diffusion Superposed on Forced Flow

The experiments which resulted in the data of Table VI were performed to verify the equations postulated for superposed flow at several different pressure drops across the septum. Specifically, it was desired to demonstrate that one could predict the individual rates through the formulae and a knowledge of the diffusion and permeability coefficients. The temperature, total pressure, and to some extent the mole

Table VI. Results of 100°C Experiments Conducted at 1.96 atm Total Pressure with Various Pressure Drops Across Septum

Pressure P (atm)	Pressure Drop $P_{He} - P_A$ (atm)	Mole Fraction of Helium		Diffusion Rates (mole/sec)			Diffusion Coefficient[a] D_{12} (cm^2/sec)
		at x=0	at x=L	$\dot{n}_{He}$	$\dot{n}_A$	$\dot{n}_T$	
	$x10^{-3}$			$x10^{-5}$	$x10^{-5}$	$x10^{-5}$	$x10^{-3}$
1.96	+3.27	0.9832	0.0672	+8.29	-1.38	+6.91	6.08
1.95	+2.77	0.9893	0.0660	+7.78	-1.50	+6.28	5.99
1.96	+2.26	0.9875	0.0614	+8.01	-1.50	+6.51	6.12
1.96	0	0.9844	0.0508	+6.63	-2.02	+4.61	6.09
1.98	-1.76	0.9834	0.0375	+5.89	-2.51	+3.38	6.49
1.95	-2.27	0.9793	0.0378	+5.62	-2.70	+2.92	6.27
1.96	-2.77	0.9782	0.0404	+5.25	-2.79	+2.46	6.14
1.96	-3.27	0.9754	0.0394	+5.00	-3.06	+1.94	6.19
1.98	-3.77	0.9747	0.0369	+4.83	-3.24	+1.59	6.21
1.97	-4.78	0.9712	0.0342	+4.60	-3.59	+1.01	6.43
1.98	-7.78	0.9596	0.0275	+3.48	-4.97	+1.49	6.58
1.98	-11.80	0.9450	0.0232	+2.40	-6.38	+3.98	6.47

a Normalized to 20°C and 1 atm by the relationship $D=D_0\left(\frac{P_0}{P}\right)\left(\frac{T}{T_0}\right)^{1.75}$.

fractions at the boundaries were held constant for the entire series. The average coefficient obtained through these experiments was the same as the average obtained through the results of the twenty-two experiments of Tables III, IV and V.

The rate data of Table VI have been plotted as closed circles on Figure 12. The general similarity between the experimental curves of Figure 5 is clearly shown with one notable exception; that is, the lack of "cross-over" points which appear on Figure 5 but not on Figure 12. The "cross-over" points are those at which the component rates change sign. In the hypothetical example, the sweep streams contained appreciable quantities of both components (see point B, Figure 2); hence, the "cross-over" points are rapidly attained as ΔP or $\dot{n}_f$ is shifted. As the sweep streams approach purity, the $\dot{n}_f$ value required to achieve "cross-over" increases markedly. "Cross-over" never occurs when the sweep gas is a pure component.

The open circles on Figure 12 represent the predicted values for each individual experiment or each set of experimental conditions. To predict a given set of rates the following steps were employed: $\dot{n}_T'$ was calculated by equation (15) using the boundary concentrations; $\dot{n}_f$ was obtained through equation (19) and the known ΔP; $\dot{n}_T$ was then known by equation (21); finally, $\dot{n}_1$ and $\dot{n}_2$ were obtained via equations (8) and

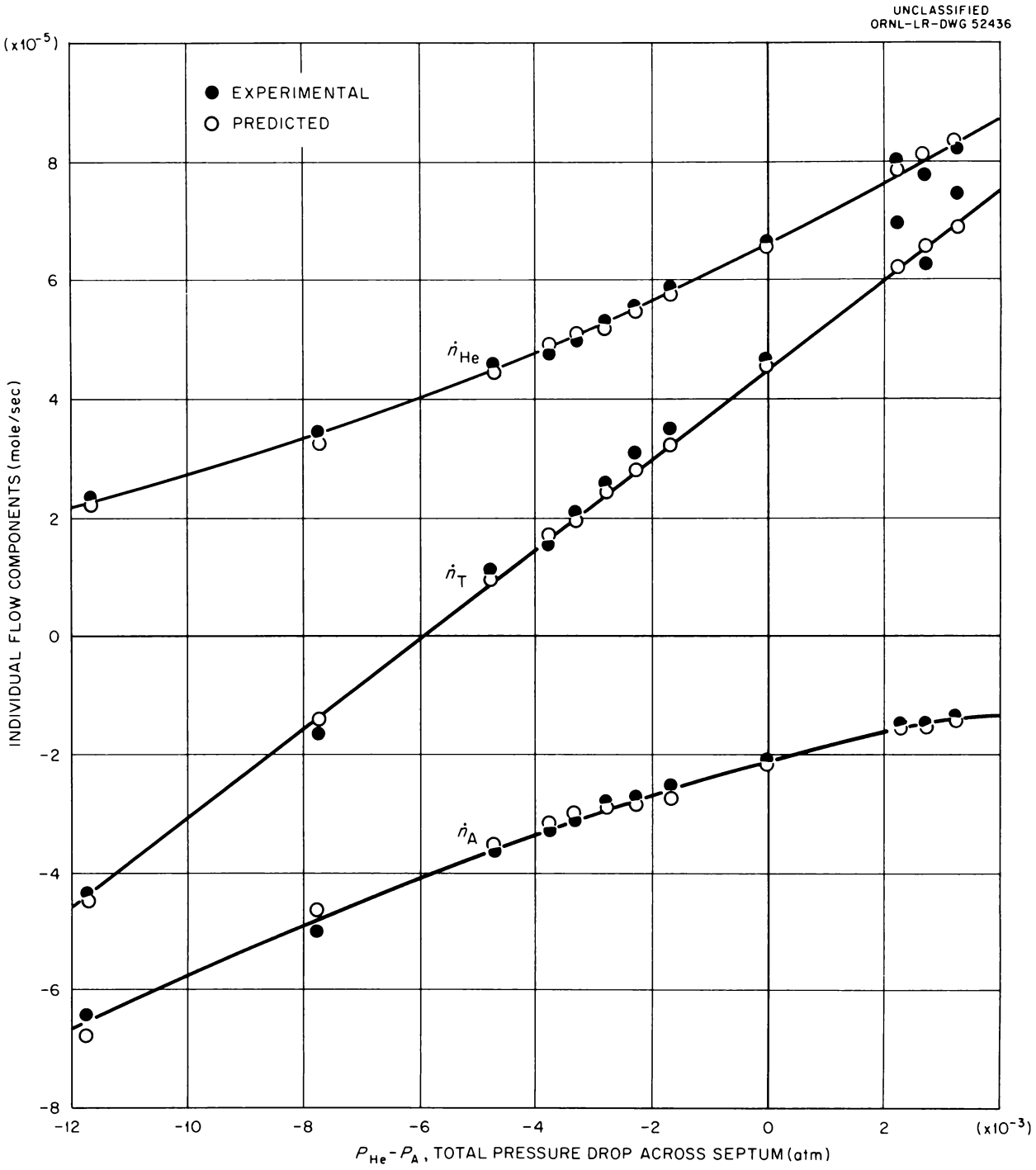

Fig. 12. Results of Diffusion Experiments at 100°C and 1.96 atm.

(9). The diffusion coefficient was obtained through the average of all the experiments of Table VI. This value was 4.84×10^{-3} cm^2/sec at 100^oC and 1.965 atm. The average permeability, K_{av}, was estimated through the graphical integration indicated by

$$\frac{1}{K_{av}} = \int_o^1 \frac{dz}{K(z)} \quad , \tag{27}$$

where

$$z = \frac{\ln r - \ln r_i}{\ln r_o - \ln r_i} \quad .$$

The $[K\ (z)]^{-1}$ versus z plot used for integration originated from a plot of K_{av} versus N_{He} (mentioned earlier) and a uniform-pressure concentration profile (N_{He} versus Z). In view of the accuracies involved, it was possible to use only one K_{av} for all calculations. The value was 1.68 cm^2/sec. A comparison of the calculated and experimental rates (open and closed circles, Figure 12) clearly shows that very good estimates of the superposed flow behavior may be made utilizing the procedures described. Thus the equations presented represent a valid model for combined diffusive and forced flow when the latter is in the viscous region and pressure diffusion effects are negligible.

To gain some insight as to the relative importance of the various parameters in an applied case it is pertinent to consider an example in which one attempts to lower the argon

concentration on the helium side by inducing considerable forced helium flow through the septum. The boundary concentrations are arbitrarily chosen as $N_{He}(0) = 1$, $N_{He}(L) = 0.9$. A combination of equations (8), (9), and (21) results in the following expression for $\dot{n}_A$,

$$\dot{n}_A = \frac{0.1\ (\dot{n}_T' + \dot{n}_f)}{\exp\left(\frac{\dot{n}_T' + \dot{n}_f}{B}\right) - 1} \tag{28a}$$

where

$$B = D\ \frac{A}{L}\ \frac{P}{RT}, \text{ and } \dot{n}_f = K\ \frac{A}{L}\ \frac{\Delta P}{RT} \quad .$$

As n_f becomes large, n_T' may be neglected. Thus,

$$\dot{n}_A \sim (0.1)\ \dot{n}_f \exp\left(\frac{-\dot{n}_f}{B}\right), \tag{28b}$$

where

$$\dot{n}_f/B = K\Delta P/P_m D \ .$$

Inspection of these equations reveals that net drift is not of importance in the "back-diffusion" process, although the net drift is important from the standpoint of experimentally determining D_{12}. Furthermore, complete sweeping of the argon is rapidly approached but is never absolute in this process.

CONCLUSIONS

1. The viscous flow region in AGOT graphite is limited to low flow rates. Transition from viscous to turbulent flow was difficult to avoid during some of the experiments.

2. The controlling mechanism for the interdiffusion of helium and argon was normal diffusion. No significant contributions could be attributed to Knudsen and/or surface diffusion effects.

3. As characterized by all normal diffusion mechanisms with binary mixtures, the Fick component of the diffusion rates could be defined by the product of the concentration gradient (of one gas) and a single mutual-diffusion coefficient.

4. The experimental system contained sources and sinks; thus, the total rate of each gas was composed of a Fick component and a net drift component. The latter was not zero at uniform total pressure.

5. The total net drift at uniform total pressure was such that the ratio of the total helium rate to that of argon was inversely proportional to the ratio of the square root of the molecular weights of the gases.

6. It was not necessary to maintain a uniform total pressure within the system in order to evaluate the mutual diffusion coefficient.

7. Diffusion equations applicable at uniform total pressure also apply when the diffusion is superposed on forced flow since the net drift for the superposed case is the sum of the net drift at uniform total pressure plus the forced flow component.

8. Although the net drift at uniform pressure is important from the standpoint of determining diffusion coefficients, it is not of importance when large forced flows of helium are used to depress back-diffusion of argon.

9. Back-diffusion of argon can be depressed by helium sweeps but the argon flow is never completely reversed.

REFERENCES

1. W. B. Cottrell et al., A Design Study of a Nuclear Power Station Employing a High-Temperature Gas-Cooled Reactor with Graphite-UO_2 Fuel Elements, ORNL-2653 (July 14, 1959).

2. H. L. Weissberg and A. S. Berman, Diffusion of Radioactive Gases Through Power Reactor Graphite, ORGDP-KL-413 (April 6, 1959).

3. GCR Quar. Prog. Rep. June 30, 1960, ORNL-2964, p. 251-2.

4. High Temperature Gas Cooled Graphite - Moderated Power Station, GA-593, GACP-595, GA-598, General Atomics, San Diego, (January 1959).

5. P. Barr, "Gaseous Flow Through Graphite and its Relations to the High Temperature Reactor System," (preprint No. 6, Q.E.E.C. High Temperature Reactor, Project - Graphite Symposium, Durley Hall, Bournemouth, November 16-19, 1959), Dragon, Windrith Heath, W. 1506, (October 1959).

6. R. D. Present, Kinetic Theory of Gases, p. 49, McGraw-Hill, New York, 1958.

7. J. Hoogschagen, J. Chem. Phys. 21, 2096 (1953).

8. K. P. McCarty and E. A. Mason, Kirkendall Effect in Gaseous Diffusion (University of Maryland), IMP-OSR-14 (June 17, 1960).

9. R. D. Present, op. cit., p. 55.

10. J. C. Maxwell and J. Stefan, cited by R. D. Present, op. cit., p. 52.

11. A. Lonius, cited by S. Dushman, Scientific Foundations of Vacuum Technique, p. 77, Wiley, New York, 1949.

12. J. O. Hirschfelder, C. F. Curtiss and R. B. Bird, Molecular Theory of Gases and Liquids, p. 519, Wiley, New York, 1954.

13. S. Chapman and T. G. Cowling, The Mathematical Theory of Non-Uniform Gases, p. 244, University Press, London, 1939.

14. J. O. Hirschfelder et al., loc. cit., p. 516.

15. M. Muskat, chap 3 in Physical Principles of Oil Production, McGraw-Hill, New York, 1949.

16. P. C. Carman, Flow of Gases Through Porous Media, p. 69, Academic Press, New York, 1956.

17. J. M. Hutcheon, B. Longstaff and R. K. Warner, "The Flow of Gases Through a Fine Pore Graphite," p. 259 in Industrial Carbon and Graphite, Soc. of Chem. Ind., London, 1957.

18. J. Truitt et al., Transport of Gases Through Ceramic Materials, ORNL-2931 (April 29, 1960).

19. W. P. Eatherly et al., "Physical Properties of Graphite Materials for Special Nuclear Applications," A/Conf. 15/p/708 (United Nations), 1958.

20. N. V. Smith and J. Truitt, EGCR Graphite Permeability Tests: Results of Forced Flow Experiments on EGCR Fuel Element Sleeves and Sleeve Material, ORNL CF-60-7-101 (July 29, 1960).

21. M. C. Cannon et al., Adsorption of Xenon and Argon on Graphite, ORNL-2955 (October 21, 1960).

22. "Standard Procedure for Determining Permeability of Porous Media," API Code No. 27, 2nd Ed., American Petroleum Institute, Division of Production, Dallas, Texas, 1942.

23. R. D. Wyckoff et al., Rev Sci. Inst. 4, 394 (1933).

24. G. L. Hassler, R. R. Rice and E. H. Leeman, Trans. Am. Inst. Mining, Met., Petrol., Engrs. 118, 116 (1936).

25. G. H. Fancher cited by M. Muskat loc. cit., p. 127.

26. H. L. Johnson and E. R. Grilley, J. Phys. Chem. 46, 957 (1942).

27. J. O. Hirschfelder et al., loc. cit., p. 562.

28. Ibid., p. 576.

29. E. Wicke, Kolloidzschr. 93, 129 (1940).

30. E. Wicke and R. Kallenbach, Kolloidzschr. 97, 135 (1941).

31. E. Wicke and U. Voigt, Angew. Chem. B19, 94 (1947).

32. A. Wheeler, "Reaction Rates and Selectivity in Catalyst Pores," Advances in Catalysis - III, p. 260-275, Academic Press, New York, 1951.

33. P. B. Weisz and C. D. Prater, "Measurements in Experimental Catalysis," Advances in Catalysis - VI, p. 185-195, Academic Press, New York, 1951.

34. P. L. Walker Jr., F. Rusinko, Jr., and E. Raats, Nature 176, 1167 (1955).

35. C. G. Rall, H. C. Hamontre and D. B. Taliaferro, "Determination of the Porosity by a Bureau of Mines Method," U.S. Bur. Mines Rl No. 5025 (July 1953).

36. P. C. Carman, op. cit. pp. 47, 51-54.

ORNL-3067
UC-4 - Chemistry
TID-4500 (16th ed.)

INTERNAL DISTRIBUTION

1. C. E. Center
2. A. M. Weinberg
3. J. A. Swartout
4. J. P. Murray
5. G. E. Boyd
6. L. B. Emlet
7. W. H. Jordan
8. C. E. Winters
9. H. G. MacPherson
10. S. C. Lind
11. J. H. Frye, Jr.
12. W. R. Grimes
13. E. H. Taylor
14. A. L. Boch
15. E. G. Bohlmann
16. A. P. Fraas
17. W. D. Manly
18. H. F. McDuffie
19. A. J. Miller
20. L. G. Alexander
21. C. J. Barton
22. M. Blander
23. F. F. Blankenship
24. W. E. Browning
25. S. Cantor
26. R. B. Evans III
27. G. W. Keilholtz
28. R. F. Newton
29. L. G. Overholser
30. W. T. Rainey
31. B. A. Soldano
32. R. A. Strehlow
33. J. A. Lane
34. R. A. Charpie
35-85. G. M. Watson
86. W. T. Ward
87. E. E. Hoffman
88. B. W. Kinyon
89. A. Taboada
90. J. S. Culver
91. C. H. Gabbard
92. P. R. Kasten
93. C. H. Secoy
94. I. Spiewak
95. M. Bender
96. W. F. Boudreau
97. F. L. Carlsen, Jr.
98. G. W. Clark
99. J. H. Coobs
100. W. B. Cottrell
101. H. N. Culver
102. J. H. DeVan
103. W. O. Harms
104. J. J. Keyes
105. W. B. McDonald
106. P. Patriarca
107. A. M. Perry
108. G. Samuels
109. A. W. Savolainen
110. J. L. Scott
111. O. Sisman
112. D. B. Trauger
113. C. S. Walker
114. H. L. Weissberg (K-25)
115. C. P. Keim
116. P. M. Reyling
117. J. Truitt
118. R. S. Cockreham
119. M. J. Skinner
120. Central Research Library
121. Reactor Division Library
122. Biology Library
123. Health Physics Library
124. Laboratory Records, ORNL R.C.
125-144. Laboratory Records Department
145. ORNL Y-12 Technical Library
146. P. H. Emmett (consultant)
147. F. T. Miles (consultant)
148. F. T. Gucker (consultant)
149. J. W. Prados (consultant)
150. E. A. Mason (consultant)
151. F. Daniels (consultant)

EXTERNAL DISTRIBUTION

152. L. Brewer, University of California
153. R. H. Condit, University of California
154. F. T. Salzano, Brookhaven National Laboratory
155. P. L. Walker, Jr., Pennsylvania State University
156. Division of Research and Development, AEC, Washington
157. Division of Research and Development, AEC, ORO
158. Division of Reactor Development, AEC, Washington
159. Division of Reactor Development, AEC, ORO
160-751. Given distribution as shown in TID-4500 (16th ed.) under Chemistry category (75 copies - OTS)